An Efficient Antibody-Catalyzed Aminoacylation Reaction

John R. Jacobsen, James R. Prudent, Lynn Kochersperger, Shirlee Yonkovich, Peter G. Schultz*

An antibody generated against a neutral phosphonate diester transition-state analog was found to catalyze the aminoacylation of the 3′-hydroxyl group of thymidine with an alanyl ester. A comparison of the apparent second-order rate constant of the antibody-catalyzed reaction [5.4×10^4 molar^{-1} minute^{-1} (M^{-1} min^{-1})] with that of the uncatalyzed reaction (2.6×10^{-4} M^{-1} min^{-1}) revealed this to be a remarkably efficient catalyst. Moreover, although the concentration of water (55 M) greatly exceeds that of the secondary alcohol, the antibody selectively catalyzes acyl transfer to thymidine. The antibody exhibits sequential binding, with Michaelis constants of 770 μM and 260 μM for acyl acceptor and donor, respectively, and a dissociation constant of 240 pM for hapten. This antibody-catalyzed reaction provides increased insight into the requirements for efficient aminoacylation catalysts and may represent a first step toward the generation of "aminoacyl transfer RNA synthetases" with novel specificities.

Acyl transfer reactions play important roles in many biological and chemical processes. For example, the esterification of the 2′,3′-diol of the terminal adenosine of tRNAs by the aminoacyl tRNA synthetases is a key step in protein biosynthesis. These enzymes have been the subject of considerable interest because of their high specificity (*1*) as well as the mechanism of the acyl transfer reaction (*2*, *3*). In order to gain greater insight into the requirements for efficient aminoacylation catalysts, we asked whether antibodies might be generated that catalyze this reaction. Moreover, such antibodies might facilitate the aminoacylation of tRNAs with novel amino acids for incorporation into proteins and studies of protein biosynthesis (*4*).

A number of acyl transfer reactions have been catalyzed by antibodies (*5*) including a remarkably efficient transesterification reaction that proceeds through an enzyme-like acyl antibody intermediate (*6*). In each case, antibodies were generated against a negatively charged phosphonate or phosphonamidate hapten. As a first step toward the generation of antibodies capable of selectively aminoacylating the acceptor stem of tRNAs, antibodies were raised against phosphonate diester **1** (Fig. 1). The phosphonate diester, in contrast to phosphonate and phosphonamidate monoesters, contains elements of the acyl donor (alanyl ester **4**), the acyl acceptor (thymidine derivative **3**), and the leaving group in a tetrahedral geometry, mimicking that of the probable transition state for the transesterification reaction (rather than that for product hydrolysis). It was anticipated that an antibody that binds both substrates in a favorable orientation would significantly accelerate the reaction by reducing the entropic barrier to reaction (*7*–*9*). Moreover, the dipole of the P=O bond reflects the developing negative charge on the carbonyl oxygen in the transition state. Antibodies complementary to tetrahedral phosphonate **1** should have considerably lower affinity for the trigonal product **10**, thereby preventing product inhibition.

Hapten **1** (mixture of diastereomers) was conjugated to the carrier protein bovine serum albumin (BSA) and keyhole limpet hemocyanin (KLH) through the activated *N*-hydroxysuccinimidyl ester (Fig. 1). The phosphonate diester was stable in serum. Thirty-nine monoclonal antibodies specific for **1** were generated by standard protocols and purified by protein A affinity chromatography as described previously (*10*). Antibody purity (>95%) was confirmed by SDS–polyacrylamide gel electrophoresis. Transesterification was assayed in 100 mM MES buffer, pH 6.5, at 26°C by monitoring product appearance using high-performance liquid chromatography (HPLC). Eight antibodies were found to accelerate the reaction of alcohol **3** with fluorophenyl ester **5** or **6** to form ester **10** or **11**, respectively. Four antibodies preferentially accelerated the reaction of L-alanine ester **5**; three were D-selective, and one demonstrated no selectivity (*11*). One L-selective catalytic antibody (18R.136.1) was characterized further.

Antibody 18R.136.1 showed no change in specific activity after further purification with a MONO-S ion-exchange column. This antibody catalyzed the reaction of alcohol **3** with phenyl ester **4** and cyanomethyl ester **7** with similar rates. No catalysis was observed with ethyl ester **9**. The reaction with cyanomethyl ester **7** was studied further because of the greater solubility of this substrate in water. Lineweaver-Burk plots were constructed by holding one substrate concentration constant while varying the concentration of the second (Fig. 2A). The slopes and y intercepts obtained from

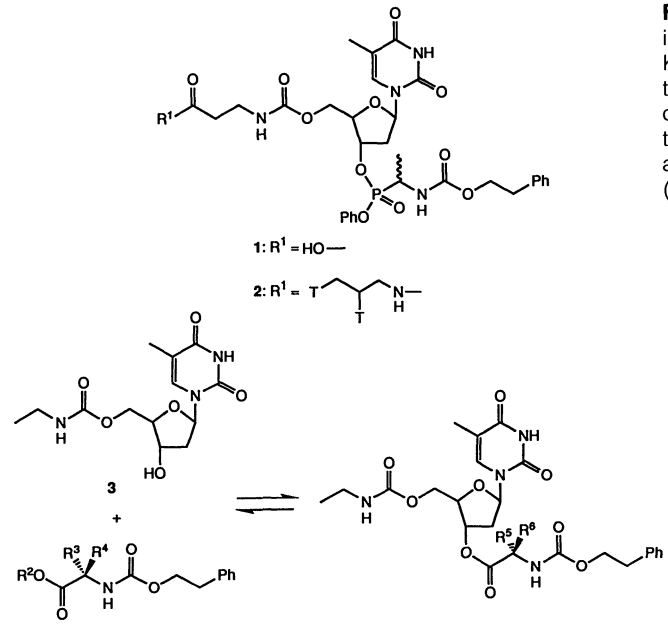

Fig. 1. Monoclonal antibodies generated against the KLH conjugate of **1** catalyze the reaction of thymidine derivative **3** with esters **4** through **8** to form aminoacylated nucleosides **10** and **11** (*18*).

J. R. Jacobsen, J. R. Prudent, P. G. Schultz, Department of Chemistry, University of California, Berkeley, CA 94720.
L. Kochersperger and S. Yonkovich, Department of Bioorganic Chemistry, Affymax Research Institute, Palo Alto, CA 94304.
*To whom correspondence should be addressed.

this analysis were replotted as a function of substrate concentration to give the true maximum rate V_{max} as 1.2 μM min^{-1} [rate constant k_{cat} = 14.2 min^{-1} per immunoglobulin (Ig)] and Michaelis constant K_m values of 770 μM and 260 μM for thymidine derivative **3** and cyanomethyl ester **7**, respectively (Fig. 2B). The apparent second-order rate constant k_{cat}/K_m is equal to 1.8×10^4 M^{-1} min^{-1} for the alcohol and 5.4×10^4 M^{-1} min^{-1} for the ester. The family of plots in Fig. 2 intersects on the horizontal axis, indicating that the antibody exhibits sequential binding (the binding of one ligand has no effect on the other). The uncatalyzed reaction of **3** with **7** was monitored by HPLC at substrate concentrations of 3.5 to 5.0 mM. Product formation was assayed after 40 to 400 min, and the second-order rate constant, k_{uncat} = 2.6×10^{-4} M^{-1} min^{-1}, showed no dependence on buffer concentration. Comparison of the uncatalyzed rate constant with that of the antibody-catalyzed reaction [$(k_{cat}/K_m)/k_{uncat} = 2.1 \times 10^8$] reveals this antibody to be a remarkably efficient catalyst.

Cyanomethyl ester **8**, derived from D-alanine, was examined as an alternative substrate at a fixed concentration of 5.0 mM thymidine derivative **3**. A Lineweaver-Burk analysis gave apparent values for k_{cat} and K_m of 0.64 min^{-1} and 340 μM, respectively. Comparison of these values with those of L-alanine derivative **7** reveals a small (1.3-fold) difference in K_m and a much larger (22-fold) difference in k_{cat}. This result suggests that antibody 18R.136.1 has low selectivity in substrate binding but discriminates the diastereomeric transition states for the transesterification reaction. This is consistent with the notion that the antibody combining site is most complementary to the transition state. A similar observation has been made in an antibody-catalyzed bimolecular imine-forming reaction (*12*).

Although the concentration of water (55 M) greatly exceeds the concentration of **3**, the antibody selectively catalyzes acyl transfer to thymidine. The hydrolysis of ester **7** was monitored in the absence of **3** by HPLC, and the first-order rate constant was 1.1×10^{-4} min^{-1}. The addition of 11 μM 18R.136.1 increases the rate of reaction by less than 11% (this may be due to nonspecific catalysis). The ability of the antibody to catalyze transesterification to a secondary alcohol without concomitant hydrolysis is characteristic of a number of highly evolved enzymes that sequester reactive species from water (*13*). One mechanistic interpretation of this behavior, in lieu of a large conformational change or deep binding cavity [not typically found in antibodies (*14*)], is that the amino acid ester is only forced into a transition-state geometry in the presence of thymidine derivative **3**. In the absence of **3**, the binding site may be able to accommodate the sp^2 planar ground state of the amino acid ester.

The antibody-catalyzed reaction is inhibited by hapten **1** as well as by product **10**. The binding of 18R.136.1 to product **10** was measured by fluorescence quenching, and a dissociation constant (K_d) of 18 nM was determined by Scatchard analysis (Fig. 3A). The rate of dissociation of the antibody-product complex was measured by performing rapid dilution of an Ig·**10** solution and observing the change in fluorescence with a stopped-flow apparatus. This afforded a rate constant for dissociation (k_{off}) of 1.5 s^{-1}, indicating that a chemical step rather than product dissociation is rate-determining in this antibody-catalyzed reaction.

The affinity of 18R.136.1 for hapten **1** was too high to be measured by fluorescence quenching. We prepared a radiolabeled ligand for the antibody by coupling allyl amine to hapten **1** through an amide bond and subsequent reduction of the double bond with tritium gas. The K_d was 240 pM (Fig. 3B). Consequently, the differential binding affinity of the antibody to phosphonate diester relative to substrates appears to account

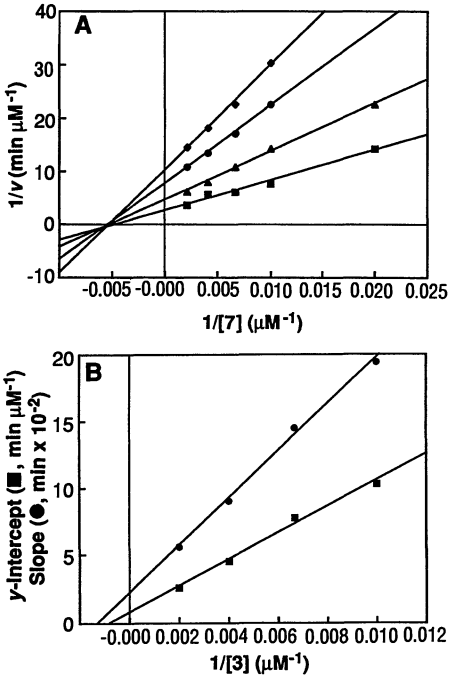

Fig. 2. (**A**) Lineweaver-Burk plot with thymidine derivative **3** held at four fixed concentrations while ester **7** was varied over concentrations ranging from 50 to 500 μM (◆ [**3**] = 100 μM; ● [**3**] = 150 μM; ▲ [**3**] = 250 μM; ■ [**3**] = 500 μM); *v*, velocity. An analogous plot was constructed with ester **7** held at fixed concentrations. Reaction mixtures contained 87 nM antibody, 10% (v/v) dimethyl sulfoxide, and 100 mM MES, pH 6.5, and were incubated at 26°C. Reactions were followed by HPLC with a Microsorb C8 reversed-phase column (Rainin Instruments) and a gradient of 35 to 65% acetonitrile in 25 mM Hepes, pH 7.5. Reaction components were detected by UV absorbance at 268 nm. Product **10** was identified by coinjection with an authentic sample and quantified against an internal standard of 6-nitroquinoline. Initial rates were determined by linear fitting of the observed product concentration at five or more time points ranging from 1 to 20 min. (**B**) Replot of *y* intercepts and slopes of Lineweaver-Burk plots as a function of $[\mathbf{3}]^{-1}$. Analogous plots were constructed to give kinetic constants for ester **7**.

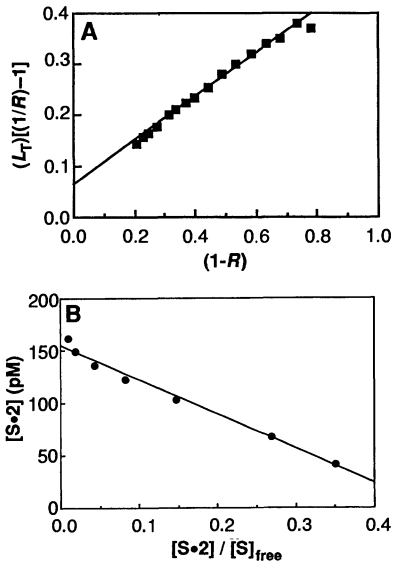

Fig. 3. (**A**) Scatchard plot for the binding of product **10** to antibody 18R.136.1, where *R* is the fraction of antibody sites that contain bound **10** and L_T is the total (bound + free) concentration of ligand **10**. Fluorescence quenching was measured in 100 mM MES, pH 6.5, 26°C. The sample was excited at 280 nm, and fluorescence was detected at 348 nm. Data were analyzed according to the method of Taira and Benkovic (*20*). We determined the rate constant for dissociation of the antibody · product **10** complex by stopped-flow fluorescence spectrometry, using an Applied Photophysics model SF.17MV instrument equipped with a 150-W xenon arc lamp. Samples were excited at 280 nm, and fluorescence was detected at >320 nm. Solutions containing antibody · product complex in 100 mM MES, pH 6.5, 26°C, were diluted 1:1 with buffer, and the change in fluorescence was measured from 10 ms to 1 s. We determined relaxation rates by fitting the observed change in fluorescence to an exponential function. Data were analyzed according to the method of Pecht *et al.* (*21*). (**B**) Eadie plot (*22*) for the binding of hapten **2** to antibody 18R.136.1, where $[\mathbf{S}]_{free}$ is the concentration of unoccupied antibody binding sites and [**S·2**] is the concentration of occupied binding sites. Reaction mixtures containing varying amounts of antibody 18R.136.1 and radiolabeled hapten **2** in 100 mM MES, pH 6.5, 26°C, were mixed with a suspension containing activated charcoal which had been blocked with bovine serum. The mixtures were centrifuged, and the hapten remaining in solution (antibody-bound) was determined by liquid scintillation.

for a large fraction of the catalytic advantage in this reaction (*15*), consistent with the classic notion of transition-state complementarity of Haldane (*16*) and Pauling (*17*).

This behavior is in contrast to that of an antibody-catalyzed transesterification reaction recently reported by Lerner and co-workers (6) (in which the antibody was raised to a negatively charged phosphonate monoester rather than a neutral phosphonate diester). This antibody-catalyzed reaction, which has a similar rate of acceleration and which also showed high specificity for the acyl acceptor versus water, proceeds through a ping-pong mechanism involving a covalent antibody · substrate complex. Thus, the tremendous diversity of the immune system has provided two mechanistic alternatives for similar acyl transfer reactions, in much the same way that enzymes have evolved with similar catalytic properties but different mechanisms (such as the acid, serine, and Zn^{2+} proteases). Further characterization of these catalytic antibodies should provide additional insight into the essential requirements for efficient acyl transfer catalysts as well as optimal hapten structures for generating such catalysts.

REFERENCES AND NOTES

1. P. Schimmel, *Annu. Rev. Biochem.* **56**, 125 (1987).
2. A. R. Fersht, R. J. Leatherbarrow, T. N. C. Wells, *Trends Biochem. Sci.* **11**, 321 (1986).
3. A. R. Fersht, *Biochemistry* **26**, 8031 (1987).
4. J. A. Ellman, D. Mendel, P. G. Schultz, *Science* **255**, 197 (1992); C. J. Noren, S. J. Anthony-Cahill, M. C. Griffith, P. G. Schultz, *ibid.* **244**, 182 (1989).
5. R. A. Lerner, S. J. Benkovic, P. G. Schultz, *ibid.* **252**, 659 (1991); P. G. Schultz, *Angew. Chem. Int. Ed. Engl.* **28**, 1283 (1989).
6. P. Wirsching, J. A. Ashley, S. J. Benkovic, K. D. Janda, R. A. Lerner, *Science* **252**, 680 (1991).
7. T. C. Bruice and U. K. Pandit, *J. Am. Chem. Soc.* **82**, 5858 (1960); M. I. Page and W. P. Jencks, *Proc. Natl. Acad. Sci. U.S.A.* **68**, 1678 (1971); D. R. Storm and D. E. Koshland, *J. Am. Chem. Soc.* **94**, 5805 (1972).
8. D. Y. Jackson, M. N. Liang, P. A. Bartlett, P. G. Schultz, *Angew. Chem. Int. Ed. Engl.*, in press.
9. S. J. Benkovic, A. D. Napper, R. A. Lerner, *Proc. Natl. Acad. Sci. U.S.A.* **85**, 5355 (1988).
10. J. Jacobs, R. Sugasawara, M. Powell, P. G. Schultz, *J. Am. Chem. Soc.* **109**, 2174 (1987).
11. Selectivity for L- or D-alanyl esters was determined by HPLC analysis of product ratios with authentic products used for comparison.
12. A. G. Cochran and P. G. Schultz, *J. Am. Chem. Soc.* **113**, 6670 (1991).
13. D. L. Pompliano, A. Peyman, J. R. Knowles, *Biochemistry* **29**, 3186 (1990).
14. D. R. Davies, E. A. Padlan, S. Sheriff, *Annu. Rev. Biochem.* **59**, 439 (1990).
15. From transition-state theory (*9, 23*)

$$\frac{K_{Ab}^{\neq}}{K_N^{\neq}} = \frac{K_A K_B}{K_T} = \frac{k_{Ab}}{k_N}$$

as defined in the scheme:

$$\begin{array}{ccc} & \overset{K_N^{\neq}}{} & \\ Ab+A+B & \rightleftarrows & [AB]^{\neq}+Ab \rightarrow P+Ab \\ \Updownarrow K_A K_B & & \Updownarrow K_T \\ & \overset{K_{Ab}^{\neq}}{} & \\ Ab{\cdot}A{\cdot}B & \rightleftarrows & [Ab{\cdot}A{\cdot}B]^{\neq} \rightarrow P{\cdot}Ab \end{array}$$

Substituting $K_m(3)$, $K_m(7)$, and $K_d(2)$ for K_A, K_B, and K_T, respectively, affords $K_A K_B / K_T \geq 834$ M, which can be compared with $k_{Ab}/k_N = 2.7 \times 10^4$ M [where $K_d(2)$ corresponds to the phenyl rather than the cyanomethyl leaving group and is therefore probably an upper limit].
16. J. B. S. Haldane, *Enzymes* (Longmans, Green, London, 1930), p. 182.
17. L. Pauling, *Chem. Eng. News* **24**, 1375 (1946).
18. Hapten **1** was prepared as follows: β-alanine benzyl ester was treated with phosgene to produce the isocyanate. This was combined with thymidine, and the 5′-acylated product was isolated by silica-gel chromatography (3% methanol–methylene chloride). Phenethyl alcohol was treated with phosgene to yield the chloroformate, which was quenched in aqueous ammonia. The resulting carbamate was combined with acetaldehyde and triphenylphosphite in acetic acid and heated to 90°C for 1 hour. The racemic diphenyl phosphonate was purified by recrystallization from methanol and hydrolyzed to the monolithium salt with 0.95 equivalent of lithium hydroxide in *N,N*-dimethyl formamide–H_2O. Reaction with thionyl chloride produced the phosphonyl chloride, which was combined with the thymidine derivative and one equivalent of triethylamine. The product was purified by silica-gel chromatography (3% methanol–methylene chloride), and the benzyl ester was cleaved by hydrogenolysis with 10% palladium hydroxide on carbon as a catalyst to yield hapten **1**. Carrier protein conjugates were prepared from the *N*-hydroxysuccinimide ester of hapten **1**. Epitope densities of 11 (KLH) and 12 (BSA) were determined by ultraviolet (UV) absorption (270 nm); protein concentrations were determined by the method of Lowry *et al.* (*19*). Allyl amine was coupled to hapten **1** with dicyclohexylcarbodiimide (DCC) and subsequently reduced with tritium gas to yield radiolabeled derivative **2**. Substrate **3** was prepared by treatment of thymidine with ethyl isocyanate in pyridine. The 5′-acylated product was isolated by silica-gel chromatography (5% methanol–methylene chloride). L-Alanine and D-alanine were treated with phenethyl chloroformate to yield the parent acids of compounds **4** through **11**. We prepared compounds **4**, **5**, **6**, **9**, **10**, and **11** by coupling the appropriate parent acid with the appropriate alcohol, using DCC and 4-dimethylaminopyridine. Esters **7** and **8** were prepared from the L and D parent acids by reaction with excess chloroacetonitrile. Compounds **4** through **11** were purified by silica-gel chromatography (**4** through **9**: 50% ethyl acetate–hexane; **10** and **11**: 5% methanol–methylene chloride). All compounds were characterized by nuclear magnetic resonance spectroscopy and mass spectroscopy.
19. O. H. Lowry, N. J. Rosebrough, A. L. Farr, R. J. Randall, *J. Biol. Chem.* **193**, 265 (1951).
20. K. Taira and S. J. Benkovic, *J. Med. Chem.* **31**, 129 (1988).
21. I. Pecht *et al.*, *J. Mol. Biol.* **68**, 241 (1972).
22. A. R. Fersht, *Enzyme Structure and Mechanism* (Freeman, New York, 1985).
23. W. P. Jencks, *Adv. Enzymol. Relat. Areas Mol. Biol.* **43**, 219 (1975).

24. We thank H. Morimoto of the National Tritium Labeling Facility for preparation of the radiolabeled hapten and J. Goldberg for assistance with stopped-flow fluorescence spectrophotometry. This work was supported under NIH grant AI24695. J.R.J. is supported by a Department of Education fellowship and P.G.S. is a W. M. Keck Foundation Investigator.

8 January 1992; accepted 2 March 1992

Identification of a Naturally Occurring Transforming Variant of the p65 Subunit of NF-κB

Ramaswamy Narayanan, John F. Klement, Steven M. Ruben, Kimberly A. Higgins, Craig A. Rosen*

Transcription factor NF-κB comprises two proteins, p50 and p65, that have sequence similarity to the v-*rel* oncogene. In primary hematopoietic cell populations an alternatively spliced form of NF-κB p65 mRNA was observed that encoded a protein designated p65Δ. Expression of the p65Δ cDNA in Rat-1 fibroblasts resulted in focus formation, anchorage-independent growth in soft agar, and tumor formation in athymic nude mice, effects not obtained with expression of p65 or a p65Δ mutant that contains a disruption within the transcriptional activation domain. Thus, p65Δ, which associated weakly and interfered with DNA binding by p65, may sequester an essential limiting regulatory factor or factors required for NF-κB function.

The NF-κB transcription factor complex contains the proteins p65 and p50 and participates in the induction of numerous cellular and viral genes (*1*). Both proteins are members of the *rel* family of proteins (*2, 3*). The v-*rel* oncogene causes lymphoid cell tumors in young birds (*4*). The ability either to activate or repress transcription is a feature shared by each of the known *rel*-related family members (*5*). Proteins in the *rel* family interact with DNA after dimerization through regions within the *rel* conserved domain (*2, 3, 6*).

Amino acids 222 to 231 in human NF-κB p65 are required for association of p65 with p50 and for DNA binding (6). We identified an alternatively spliced form of p65 mRNA designated p65Δ, which lacks nucleotides (nt) that encode amino acid residues 222 to 231. The prevalence of p65Δ mRNA in certain cell lineages was

R. Narayanan and K. A. Higgins, Department of Molecular Genetics, Hoffmann–La Roche, Inc., Nutley, NJ 07110.
J. F. Klement, S. M. Ruben, C. A. Rosen, Department of Gene Regulation, Roche Institute of Molecular Biology, 340 Kingsland Street, Nutley, NJ 07110.

*To whom correspondence should be addressed.